Fabrication of Quantum Dot/Polymer Composites: Phosphine-Functionalized Block Copolymers as Passivating Hosts for Cadmium Selenide Nanoclusters

D. E. Fogg,[†] L. H. Radzilowski,[‡] R. Blanski,[†] R. R. Schrock,*[,†] and E. L. Thomas[‡]

Departments of Chemistry and Materials Science and Engineering, Massachusetts Institute of Technology, Cambridge, Massachusetts 02139

Received July 25, 1996; Revised Manuscript Received November 26, 1996[⊗]

ABSTRACT: Nearly monodisperse CdSe nanoclusters, surface-passivated with a layer of trioctylphosphine and trioctylphosphine oxide, have been sequestered within phosphine-containing domains in a diblock copolymer. A convergent approach to fabrication of these composites was adopted via independent synthesis of nanoclusters and polymer. Diblock copolymers of phosphine- or phosphine oxide-functionalized monomers and methyltetracyclododecene (MTD) were prepared by ring opening metathesis polymerization using Mo alkylidene initiators. Nanoclusters were prepared by pyrolysis of $CdMe_2$ and $Se{=}P(octyl)_3$ in the presence of $P(octyl)_3$ and $O{=}P(octyl)_3$. An immediate and sustained increase in electronic passivation is found for nanoclusters incorporated into octylphosphine-containing polymers. In contrast, nanoclusters in pure hydrocarbon or phosphine oxide-containing polymers rapidly lose passivation. Films of nanoclusters in a phosphine-containing polymer matrix were static cast from dilute solution. Under suitable conditions, the copolymers underwent microphase separation, and the metal chalcogenide clusters were predominantly sequestered within the phosphine-containing microdomains. The original, highly uniform cluster size distribution was unaffected.

Introduction

Much recent effort has been directed toward the fabrication of polymers containing nanometer-sized clusters of inorganic semiconductors.[1−6] Recent advances in the synthesis of highly monodisperse CdSe nanoclusters ("quantum dots"),[7] coupled with methodologies for the preparation of ROMP polymers with very narrow molecular weight distributions,[8−11] offer an unprecedented level of control over the molecular architecture of the composite materials. Most of the reported approaches to such composites involve in situ aggregation of labile metal species within a polymer matrix. For example, organometallic−hydrocarbon diblock copolymers have been prepared by living ring-opening metathesis polymerization (ROMP) of methyltetracyclododecene (MTD) and metal-functionalized norbornene monomers.[12−14] Microphase separation, followed by hydrogenation or pyrolysis, yielded nanometer-sized particles of elemental metal within approximately spherical microdomains; cluster size was defined by the number of monomers within the metal-functionalized block. In a related approach, copolymers of MTD and donor-functionalized norbornenes were treated with labile metal species.[3,15,16] Controlled decomposition of the polymer-attached metal complex produced metal clusters distributed throughout the polymer matrix. The size of the metal clusters formed in lamellar or cylindrical microdomains typically varied in diameter by ±20%, although evidence suggests that a single cluster can form in a suitably small spherical microdomain. Uniform dispersion of nanoclusters in solid media is frequently hampered by phase separation and cluster aggregation within the matrix. In these examples dispersion is effected by the affinity of the metal for the donor groups uniformly distributed within one block.

An alternative, convergent approach is adopted in the present work, in which prefabricated clusters are incorporated within a polymer containing phosphine donors attached to the polymer backbone. This approach permits us to exploit recently developed methods for the preparation of CdSe quantum dots with remarkably narrow size distributions (<5% rms in diameter).[7] Novel optical properties are conferred on the composites as a result of the uniform, small particle size. The length scale of the clusters (maximum diameter ∼50 Å) is smaller than the Bohr diameter of the exciton in bulk CdSe (112 Å), leading to three-dimensional quantum confinement of photogenerated electron−hole pairs. Quantum confinement results in the appearance of discrete absorption bands, blue-shifted relative to bulk CdSe (for which the excited states form a continuum). The extent of the shift is very sensitive to cluster size, and visible absorption spectroscopy provides a useful probe of both cluster size and the size distribution.

A further, fundamental advance in these materials lies in the luminescent properties of the clusters. Electronic passivation of the nanoclusters is effected by saturating the cluster surface with bulky trioctylphosphine/trioctylphosphine oxide groups, thus preventing localization of the carriers in trap states, and sterically enforcing segregation of the clusters. The resulting overlap between the electron and hole wavefunctions of the exciton leads to a high rate of radiative recombination, and quantum yields of up to 10% are observed in room-temperature fluorescence experiments.[7]

Our principal interest to date has focused on the development of suitable donor-functionalized monomers and optimization of their polymerization, as well as the cluster-sequestering ability of the resulting polymers. In principle, the properties of the host polymer (either in a random or block copolymer) can be tailored for the intended application. For example, the photoelectronic properties of uniformly dispersed nanoclusters could be exploited to provide electronic devices within a conductive polymer matrix. In this work we report the

[†] Department of Chemistry.
[‡] Department of Materials Science and Engineering.
[⊗] Abstract published in *Advance ACS Abstracts,* January 15, 1997.

S0024-9297(96)01103-5 CCC: $14.00

development of copolymers that contain phosphine- and phosphine oxide-functionalized norbornene blocks. Quantitative uptake of trioctylphosphine/phosphine oxide-capped CdSe quantum dots by these materials is described. In the case of the phosphine-functionalized polymers, excellent retention of the narrow size distribution of the clusters is found. Fluorescence is enhanced, indicating an increase in electronic passivation in the donor matrix. Transmission electron microscopy (TEM) examination of thin films of the composites reveals segregation of the clusters within an extended network of phosphine-rich domains. Samples microtomed from the bulk show segregation into spherical microdomains. We are currently exploring the potential of these materials for exciton delocalization and charge transport. Future work will focus on synthesis of copolymers containing electron- and hole-carrier segments, for the development of new materials for electroluminescence applications.

Experimental Section

General. All experiments, unless otherwise noted, were performed under a nitrogen atmosphere in a Vacuum Atmosphere drybox or by using standard Schlenk/vacuum line techniques. Hexanes, diethyl ether, and tetrahydrofuran (THF) for polymerization were distilled from purple sodium benzophenone ketyl under nitrogen and then stored in the drybox over activated 4 Å molecular sieves. Pentane was washed with 5% nitric acid in sulfuric acid, stored over calcium chloride, and then distilled from sodium benzophenone ketyl under nitrogen. *n*-Butanol, cyclohexane, and methylene chloride were used as received. Tri-*n*-octylphosphine oxide (92%) and tri-*n*-octylphosphine were obtained from Johnson Matthey. The former was used as received, the latter was distilled under Ar prior to use. Selenium shot (1.6 mm, 99.999+%) was used as received from Johnson Matthey. Dimethylcadmium was obtained from Organometallics, Inc., purified by filtration and distillation, and stored under N_2 at −40 °C. Methyltetracyclododecene (MTD) was provided by B. F. Goodrich and was purified by vacuum distillation from sodium. 5-Norbornen-2-yl-methanol and 1,5-dibromopentane were obtained from Aldrich Chemical Co. and used as received. ROMP initiators $Mo(CHCMe_2Ph)(NAr)(O\text{-}t\text{-}Bu)_2$ (Ar = 2,6-C_6H_3-*i*-Pr_2; Ar′ = 2,6-C_6H_3-Me_2),[17] racemic NORPHOS[18] (NORPHOS = 2-*exo*-3-*endo*-bis(diphenylphosphino)bicyclo[2.2.1]heptene), and $P(NEt_2)(oct)_2$[19] were synthesized according to literature procedures. The synthesis of 2-(chloromethyl)-5-norbornene was carried out as described in the literature,[20] except at room temperature instead of reflux temperature.

Nuclear magnetic resonance (NMR) spectra were recorded on a Varian XL301 (300.0 MHz for ^1H, 121.4 MHz for ^{31}P) FT-NMR spectrometer. Proton spectra were measured in C_6D_6 unless otherwise noted; data are listed in parts per million downfield from tetramethylsilane and referenced against the residual proton signals from the deuterated solvent (δ 7.16, C_6D_6) as internal standard. ^{31}P NMR spectra are referenced against 85% H_3PO_4 as an external standard. Downfield shifts are taken as positive for all nuclei. Gel permeation chromatographic (GPC) analysis was carried out at room temperature employing a Rheodyne Model 7125 sample injector, a Kratos Spectroflow 408 pump, two Jordi-Gel DVB mixed bed columns in series, and a Viscotek differential refractometer/viscometer H-500 on samples 0.1−0.3% (w/v) in THF, which were filtered through a Millex-SR 0.5 μm filter in order to remove particulates. GPC columns were calibrated versus commercially available polystyrene standards (Polymer Laboratories Ltd.) ranging from 1206 to 1.03×10^6 MW. Fluorescence experiments were performed on a SPEX Fluorolog-2 spectrometer, using front face collection with 0.4 mm slits. Fluorescence spectra for ∼37 Å clusters (absorbance λ_{max} 536 nm) were collected between 480 and 600 nm with 436 nm excitation, and for ∼45 Å clusters (absorbance λ_{max} 578 nm), between 530 and 640 nm with 478 nm excitation. Optical absorption spectra were obtained at room temperature on a Hewlett-Packard 8452A diode array spectrometer, using 1 cm quartz cuvettes. Transmission electron microscopy (TEM) was performed on a JEOL 200 CX in bright field at 100 kV.

Nanocluster Synthesis. CdSe quantum dots were prepared by pyrolysis of $CdMe_2$ and $Se{=}P(oct)_3$ (oct = octyl) in the presence of $P(oct)_3$ and its oxide, as described by Murray et al.[7] Slightly higher temperatures (330 °C) were employed. Size-selection was effected by three cycles of reprecipitation from ^{n}BuOH−hexanes (5:1) by dropwise addition of MeOH. Clusters were dried in vacuo and stored under N_2 in a drybox.

$PCl(oct)_2$. Ethereal HCl (1 M, 335 mL) was added dropwise to an ice-cold solution of $P(NEt_3)(oct)_2$ (50 g, 0.152 mol) in diethyl ether (300 mL). The mixture was allowed to warm to room temperature. It was checked for acidity, filtered through Celite in order to remove diethylamine hydrochloride, and then stripped to dryness. The crude product was distilled to yield 27.5 g (62%) of a colorless oil (bp 128−135 °C, 0.4 Torr): ^1H NMR δ 1.21−1.51 (m, 28H, CH_2), 0.87−0.92 (t, J = 7 Hz, 6H, CH_3); $^{31}P\{^1H\}$ NMR δ 113.5 (s); $^{13}C\{^1H\}$ NMR δ 35.5 (d, J_{PC} = 28 Hz), 32.2 (s), 31.2 (d, J_{PC} = 10 Hz), 29.6 (s), 29.57 (s), 24.9 (d, J_{PC} = 12 Hz), 23.1 (s), 14.3 (s).

5-Norbornen-2-yl-$CH_2P(oct)_2$ [NBE-$CH_2P(oct)_2$, 1]. A solution of NBE-CH_2Cl (5.60 g, 39.3 mmol) in THF (2 mL) was added dropwise to a suspension of Mg powder (1.15 g, 47.1 mmol) in THF (50 mL). The solution was refluxed for 3 h, cooled, and filtered through Celite in the drybox. Titration against MeOH (1,10-phenanthroline indicator) indicated 28.3 mmol of active Grignard, which was added to a chilled solution of $PCl(oct)_2$ (8.285 g, 28.3 mmol) in THF (40 mL). The solution was stirred for 12 h and then stripped of solvent and extracted with pentane. The pentane extract was filtered, stripped, and distilled to yield 9.1 g (64%) of **1** as a colorless oil (bp 150 °C, 0.1 Torr): ^1H NMR δ (endo isomer, ∼80%) 6.11−6.13 (m, 1H, olefinic), 6.04−6.07 (m, 1H, olefinic), 2.94 (br s, 1H, bridgehead CH), 2.67 (br s, 1H, bridgehead CH), 2.1−2.23 (m, 1H, exo CH), 1.94−1.98 (m, 1H, exo CH of CH_2), 1.17−1.57 (m, 32H, CH_2), 0.88−0.92 (m, 6H, CH_3), 0.68−0.78 (m, 1H, endo CH of CH_2); (exo isomer, partial) 5.94−6.0 (m, 1H, olefinic), 2.71 (br s, 1H, bridgehead CH); $^{31}P\{^1H\}$ NMR δ −35.3 (s, exo), −35.7 (s, endo).

5-Norbornen-2-yl-$CH_2P(O)(oct)_2$ [NBE-$CH_2P(O)(oct)_2$, 2]. A solution of 30% aqueous H_2O_2 (3.7 mL, 33 mmol) was added dropwise to ice-cooled **1** (6.0 g, 16.5 mmol) in CH_2Cl_2 (50 mL) in air. The solution was stirred for 2 h and then stripped of solvent. The crude, pale yellow product was distilled to give 5.6 g (90%) of **2** as a colorless oil (bp 180 °C, 0.03 Torr): ^1H NMR δ (endo isomer, ∼80%) 6.09 (m, 1H, olefinic), 6.03−6.04 (m, 1H, olefinic), 2.99 (br s, 1H, bridgehead CH), 2.63 (br s, 1H, bridgehead CH), 2.34−2.50 (m, 1H, exo CH), 1.88−1.95 (m, 1H, exo CH of CH_2), 1.1−1.6 (m, 32H, CH_2), 0.87−0.92 (m, 6H, CH_3), 0.55−0.63 (m, 1H, endo CH of CH_2); (exo isomer, partial) 5.91−5.98 (m, 1H, olefinic), 2.71 (br s, 1H, bridgehead CH), 2.74 (br s, 1H, bridgehead CH); $^{31}P\{^1H\}$ NMR (121 MHz, C_6D_6) δ 49.6 (s, exo), 49.8 (s, endo); $^{13}C\{^1H\}$ NMR δ (endo isomer) 138.4, 133.1 (C olefinic), 50.2, 48.1, 43.6, 43.1, 34.8, 32.6, 31.9, 30.0, 29.9, 23.5, 22.4, 14.7; (exo isomer, partial) 137.5, 137.1 (C olefinic), 50.1, 49.4, 45.9, 39.9, 34.3, 33.4, 30.5, 29.6, 29.4, 28.7, 28.5, 27.0.

5-Norbornen-2-yl-$CH_2O(CH_2)_5Br$ [NBE-$CH_2O(CH_2)_5Br$, 3]. Aqueous NaOH (50% w/w, 195 g) was added to a mixture of 5-norbornene-2-methanol (50.7 g, 0.408 mmol) and 1,5-dibromopentane (169.1 g, 0.735 mol) in cyclohexane (400 mL) in air. Aliquat, $CH_3N[(CH_2)_7CH_3]_3^+Cl^-$ (9.5 g, 23.5 mmol), was added as phase-transfer catalyst, and the mixture stirred for 9 days, or until no unreacted alcohol was observable by ^1H NMR. The organic layer was then separated, washed with H_2O (3 × 100 mL), dried over $MgSO_4$, and stripped of solvent. Fractional distillation under vacuum gave 62.3 g (56%) of a clear, colorless oil (bp 125−130 °C, 0.15 Torr) after removal of unreacted dibromopentane (bp 65−70 °C, 1 Torr): ^1H NMR δ (endo isomer, ∼80%) 6.04−6.09 (m, 1H, olefinic), 5.86−5.88 (m, 1H, olefinic), 2.93−3.42 (m, 6H, CH_2), 2.86 (br s, 1H, bridgehead CH), 2.74 (br s, 1H, bridgehead CH), 2.26−2.31 (m, 1H, exo CH), 1.18−1.89 (m, 9H, CH_2), 0.41−0.47 (m, 1H, endo CH of CH_2); (exo isomer, partial) 6.01−6.02 (m, 1H, olefinic), 2.70 (br s, 1H, bridgehead CH); $^{13}C\{^1H\}$ NMR δ (endo

Table 1. Physical Data for Polymers

polymer[a]	% yield	MW (theory)	M_n (found)	PDI[b]
$[MTD]_{300}$	96	52 500	70 800	1.06
$[MTD]_{300}[NORPHOS]_{20}$	98	61 800	35 700	1.16
$[MTD]_{300}[NBE\text{-}CH_2P(O)(oct)_2]_{20}$	81	59 800	75 000[c]	1.93
			2 034 000	1.59
$[MTD]_{300}[NBE\text{-}CH_2O(CH_2)_5P(oct)_2]_{20}$	98	61 500	53 000[d]	1.05
			795 200	1.03
$[MTD]_{300}[NBE\text{-}CH_2O(CH_2)_5P(O)(oct)_2]_{20}$	87	61 800	81 000	1.07
			135 000[e]	1.03

[a] All polymers were prepared in THF, using $Mo(CHMe_2Ph)(NAr)(O\text{-}t\text{-}Bu)_2$ as initiator. Theoretical MW values are based on 100% conversion of monomer and complete consumption of initiator, allowing for $PhMe_2CCH=$ and $=CHPh$ end groups. M_n (found) was determined by viscometry relative to polystyrene standards. [b] Polydispersity index, M_w/M_n. [c] Main peak of bimodal trace; approximate relative area 6.5:1. [d] Main peak of bimdoal trace; approximate relative area 12:1. [e] Main peak of bimodal trace; approximate relative area 2:1.

isomer) 136.8, 132.2 (C olefinic), 49.3, 43.9, 42.1, 38.7, 33.7, 32.6, 29.1, 28.8, 24.9; (exo isomer, partial) 136.3 (C olefinic), 44.9, 43.6, 41.5, 38.8, 29.7. Anal. Calcd for $C_{13}H_{21}BrO$; C, 57.15; H, 7.75. Found: C, 57.16; H, 8.01.

5-Norbornen-2-yl-$CH_2O(CH_2)_5P(oct)_2$ [NBE-$CH_2O(CH_2)_5P(oct)_2$, 4]. Neat **3** (10.0 g, 36.6 mmol) was added dropwise to a suspension of powdered Mg (1.20 g, 49.4 mmol) in THF (50 mL) over a period of 1 h and the addition funnel was rinsed with a small quantity of THF. The solution was gently refluxed for 12 h and then cooled to room temperature, brought into the glovebox, and filtered through Celite. The resulting yellow-brown Grignard reagent was titrated as for **1**. The solution was cooled to −40 °C, and neat $PCl(oct)_2$ (10.72 g, 36.6 mmol) was added dropwise. The solution was stirred for 3 h, filtered through Celite to remove $MgCl_2$, and stripped of solvent. The residue was taken up in pentane, refiltered, and stripped to a colorless oil (15.6 g, 94%). The product was purified by chromatography on neutral Al_2O_3 (hexanes eluant) and distillation (bp 220 °C, 0.03 Torr) to yield 11.4 g (69%): ^1H NMR δ (endo isomer, ∼80%) 6.03−6.06 (m, 1H, olefinic), 5.93−5.98 (m, 1H, olefinic), 2.95−3.34 (m, 7H, CH_2 and bridgehead CH), 2.64 (br s, 1H, bridgehead CH), 2.36−2.38 (m, 1H, exo CH), 1.11−1.74 (m, 37H, CH_2), 0.87−0.91 (m, 6H, CH_3), 0.41−0.47 (m, 1H, endo CH of CH_2); (exo isomer, partial) 2.82 (br s, 1H, bridgehead CH), 2.68 (br s, 1H, bridgehead CH); $^{31}P\{^1H\}$ NMR δ −31.9 (s); $^{13}C\{^1H\}$ NMR δ (endo isomer) 136.9, 132.0 (C olefinic), 49.2, 49.1, 43.7, 43.3, 41.9, 41.3, 38.5, 33.5, 33.1, 32.3, 31.6, 28.8, 28.6, 28.5, 26.5, 24.6, 23.8, 19.4, 13.4; (exo isomer, partial) 136.3 (C olefinic), 44.7, 44.6, 43.4, 43.0, 41.5, 41.2, 38.6, 31.7, 31.5, 31.4, 29.5, 29.3, 29.2, 26.6, 12.3.

5-Norbornen-2-yl-$CH_2O(CH_2)_5P(O)(oct)_2$ [NBE-$CH_2O(CH_2)_5P(O)(oct)_2$, 5]. Aqueous H_2O_2 (7.5 g, 33 mmol, 30% (w/w)) was added drop-wise to a solution of crude **4** (15.0 g, 33.3 mmol) in CH_2Cl_2 (50 mL) at room temperature. The mixture was stirred for 5 h and then partitioned between CH_2Cl_2 and water. The organic layer was dried ($MgSO_4$), stripped, and chromatographed on neutral Al_2O_3, eluting initially with neat hexanes and then with 5% acetone−hexanes. The colorless product was distilled under vacuum (235 °C, 0.03 Torr) to yield 8.6 g (55%): ^1H NMR δ (endo isomer, ∼80%) 6.0−6.1 (m, 1H, olefinic), 5.93−5.98 (m, 1H, olefinic), 2.90−3.32 (m, 7H, CH_2 and bridgehead CH), 2.63 (br s, 1H, bridgehead CH), 2.26−2.38 (m, 1H, exo CH), 1.1−1.8 (m, 37H, CH_2), 0.8−0.95 (m, 6H, CH_3), 0.4−0.5 (m, 1H, endo CH of CH_2); (exo isomer, partial) 2.8 (br s, 1H, bridgehead CH), 2.68 (br s, 1H, bridgehead CH); $^{31}P\{^1H\}$ NMR δ 44.2 (s); $^{13}C\{^1H\}$ NMR δ (endo isomer)136.6, 132.3 (C olefinic), 49.2, 44.0, 42.1, 38.8, 31.7, 31.1, 31.0, 29.3, 29.1, 28.4, 27.5, 22.6, 21.7, 13.8; (exo isomer, partial) 136.4 (C olefinic), 44.9, 43.8, 41.5, 39.0, 29.5, 29.0, 27.9, 27.7, 21.6, 21.5. Anal. Calcd for $C_{29}H_{55}O_2P$; C, 74.63; H, 11.88. Found: C, 74.49; H, 11.98.

Reaction of Phosphine Monomers with Mo Initiators. (a) NBE-$CH_2P(oct)_2$ (1, 5 equiv) + $Mo(NAr)(CHCMe_2Ph)(O\text{-}t\text{-}Bu)_2$ (6). A solution of **6** (5 mg, 9 μmol) in C_6D_6 (0.5 mL) was added to a solution of **1** (17 mg, 47 μmol) in C_6D_6 (0.5 mL): ^1H NMR δ 13.2 (m), 12.83 (m), 12.6 (m), 6.04−6.13 (m, olefinic, **1**), 5.6 (m, ring-open olefin); $^{31}P\{^1H\}$ NMR δ 31.4 (s), 28.4 (s), 21.9 (s), 21.4 (s), −34.9 (s, exo **1**), −35.8 (s, endo **1**).

(b) NBE-$CH_2P(O)(oct)_2$ (2, 5 equiv). A solution of **6** (5 mg, 9.1 μmol) in C_6D_6 (0.5 mL) was added to **2** (18 mg, 48 μmol): ^1H NMR δ 5.6 (br m, ring-open olefin); $^{31}P\{^1H\}$ NMR δ 49.6 (s), 50 (s).

(c) NBE-$CH_2O(CH_2)_5P(oct)_2$ (4, 5 equiv). A solution of **6** (1.0 mg, 1.8 μmol) in C_6D_6 (0.5 mL) was added to a solution of **4** (4 mg, 9 μmol) in C_6D_6 (0.2 mL). Monitoring of the reaction by ^1H NMR indicated complete consumption of monomer within 1 h: ^1H NMR δ 5.6 (br m, ring-open olefin); $^{31}P\{^1H\}$ NMR δ −31.9 (s).

General Procedure for Polymer Synthesis. The synthesis of the $[MTD]_{300}[NBE\text{-}CH_2O(CH_2)_5P(oct)_2]_{20}$ diblock copolymer (see Table 1), is given as an example. (The numerical subscripts following the monomer name indicate the number of equivalents of a monomer that are added to 1 equiv of the alkylidene initiator. Previous studies with these initiators have shown that in many cases the number of equivalents added approximately equal the actual degree of polymerization of the individual blocks[21]). A solution of $Mo(CHCMe_2Ph)(NAr)(O\text{-}t\text{-}Bu)_2$ **6** (1.0 mg, 1.82 μmol) in THF (1 mL) was added all at once to a rapidly stirred solution of MTD (95 mg, 0.545 mmol) in THF (7 mL). After 1 h, a solution of NBE-$CH_2O(CH_2)_5P(oct)_2$ (16.4 mg, 36.4 μmol) in THF (2 mL) was added, and the mixture stirred for 2 h before quenching by addition of 3 drops of PhCHO. The solution was stirred for 2 h and then reduced in volume to 1 mL and added dropwise to degassed MeOH (20 mL). The white solid was collected by filtration, washed with MeOH, and dried under high vacuum for 24 h to yield 104 mg (93%).

Extent of Incorporation of CdSe Nanoclusters into Polymers. In a representative experiment, a solution of $[MTD]_{300}$ (50 mg) in THF (2.0 mL) was added to a solution of the nanoclusters (10 mg) in THF (1 mL). The mixture was stirred for 1 h and the solvent was removed in vacuo. Extraction of the residue with 10 mL of pentane yielded a pale orange solution, which was diluted to 2.0 mL. The UV−visible spectrum of the solution was measured and the concentration of nanoclusters in solution calculated by interpolation against a Beer's law plot for the polymer-free nanoclusters.

Preparation of Samples for TEM Analysis. Samples were prepared from solution-cast films in two different ranges of thickness: thin films (< 100 nm) and bulk films (0.1 to 1 mm). For thin films, typically 0.84 mg (42 μL of a 20 mg/mL solution) of copolymer in THF was diluted with 1.8 mL of THF. A solution of the nanoclusters (170 μL of a 1 mg/mL solution in THF) was added to give 20% w/w cluster to polymer, and a final concentration of 0.05 wt % polymer relative to THF. The solution was allowed to equilibrate for 24 h. Films were then cast by dropping ∼100 μL of the solution onto cleaved mica coated with ∼10 nm of evaporated carbon. The rate of solvent evaporation from the cast solution was reduced by addition of 3 mL of THF to the casting chamber, which was covered and left to stand. After drying (typically within 24 h) and removing from the drybox, pieces of the carbon/polymer composite films were floated onto deionized water and picked up with 200 mesh copper TEM grids. Film thicknesses were estimated to be in the range of 30−50 nm based on their silver interference color when floating on water. Thin films were also studied in cross section. Sample-containing grids (as prepared above) were first coated with approximately 2 nm of evaporated carbon on both sides, embedded in MedCast epoxy, and then cured at 70 °C overnight. The carbon coating simultaneously prevents

Scheme 1. Routes to Dioctylphosphine- and Phosphine Oxide-Functionalized Norbornene Monomers

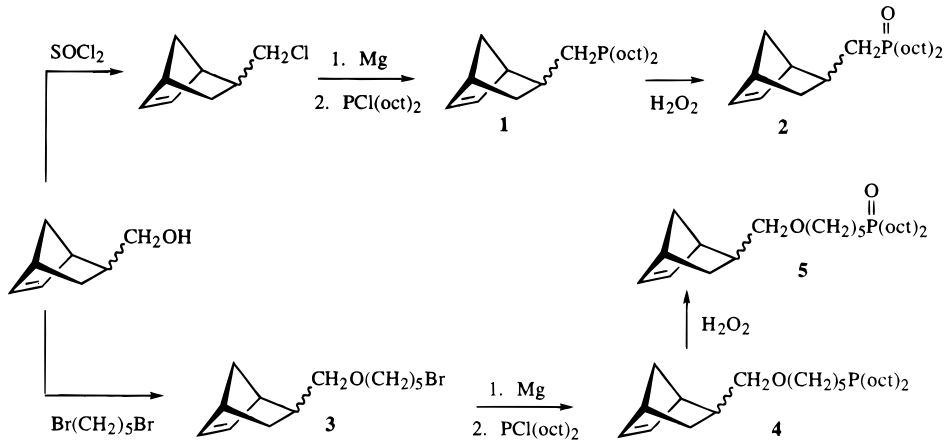

swelling of the copolymer film by the uncured epoxy and enhances adhesion at the epoxy−specimen interface. Cross sections were made by cutting directly through the embedded sample/grid in a direction normal to the grid plane using a Reichert Ultracut E ultramicrotome and a diamond knife at room temperature. The resulting sections were approximately 30−50 nm thick. Bulk films were prepared by casting a solution of 5 wt % polymer relative to THF into a ceramic crucible, covering, and keeping in a drybox until all solvent had evaporated (approximately 7 d). The resulting ~0.5 mm thick films were ultramicrotomed to give 50 nm thick sections.

Results

Synthesis of CdSe Nanoclusters. Nanoclusters with a narrow size distribution, electronically passivated by a surface layer of $P(oct)_3$ and its oxide, were prepared by the method of Murray et al. (eq 1).[7] Pyrolysis of

$$CdMe_2 + Se{=}P(oct)_3 \xrightarrow[P(oct)_3,\ \Delta]{O{=}P(oct)_3} CdSe[O{=}P(oct)_3, P(oct)_3] \quad (1)$$

dimethylcadmium and $Se{=}P(oct)_3$ at ~330 °C in the presence of $P(oct)_3$ and molten $O{=}P(oct)_3$ induces rapid and homogeneous nucleation, as indicated by an instantaneous color change from colorless to orange.

A sharp drop in temperature (~100 °C) accompanies initial nucleation. Subsequent growth and annealing of the initially formed clusters are effected by reheating, during which the size of the nanoclusters is monitored by visible spectroscopy. The rate of reheating is critical to maintaining a narrow size distribution. Too rapid a temperature rise permits formation of new nucleation sites, while too slow a rate permits aggregation of smaller clusters. In either case the principal absorption band broadens, and secondary absorption features lose definition or disappear altogether. Refinement of the size distribution and removal of solvating phosphine/phosphine oxide is effected by three cycles of reprecipitation (beyond which loss of the passivating layer occurs, and fluorescence is diminished). Clusters were dried in vacuo and stored under N_2 in a drybox, as decreased fluorescence was found on prolonged exposure of the clusters to air in the solid state, or overnight in solution. Cluster degradation by oxidation of Se surfaces to SeO_2 on exposure to air has been described in related work.[22]

Excellent retention of fluorescence is found for THF solutions of $CdSe[O{=}P(oct)_3,P(oct)_3]$ nanoclusters made up and stored in the drybox for up to 1 week. An unexpected complication arising from this protocol is an observed increase in fluorescence intensity as air diffuses into solution. The cause of this increase is still unclear, but the high oxygen-sensitivity of these measurements requires rigorous exclusion of air in all comparative fluorescence experiments conducted under initially anaerobic conditions, such as the passivation and some of the polymer-incorporation experiments described below. Experiments conducted under aerobic conditions need only be corrected for volume before emission is remeasured, but are limited to immediate comparative measurements.

Monomer Synthesis and Properties. Three classes of phosphine-substituted norbornene monomers were investigated. One is the commercially available diphosphine NORPHOS, while the other two are dioctylphosphine derivatives of 5-norbornene-2-methanol. (All such 2-substituted-5-norbornenes will be abbreviated as NBE-R throughout the rest of this paper.) The phosphine-containing monomers are the following:

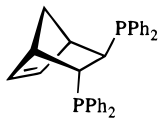

NORPHOS

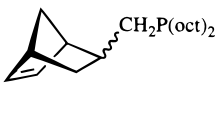

NBE-$CH_2P(oct)_2$ (**1**)

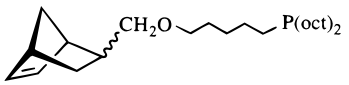

NBE-$CH_2O(CH_2)_5P(oct)_2$ (**4**)

Routes to **1** and **4** are shown in Scheme 1. NBE-CH_2Cl and NBE-$CH_2O(CH_2)_5Br$ (**3**), prepared by reaction of the norbornyl alcohol precursor with $SOCl_2$ or 1,5-dibromopentane, respectively, were converted to their Grignard derivatives and then treated with $PCl(oct)_2$ to generate the desired phosphines. The chlorophosphine itself is prepared by acid deamination of $Et_2NP(oct)_2$.[19] All norbornene derivatives are obtained as mixtures of endo and exo isomers, which are not separated. For **1**, two singlets are observed by ^{31}P NMR in a ratio of ~4.5:1. The upfield singlet (δ −35.3) is assigned to the exo isomer; the downfield signal (δ −35.7) to the predominant endo species. For **4**, in which the phosphorus atom is further from the endo/exo center, only one ^{31}P NMR signal is observed. The phosphine oxides [NBE-$CH_2P(O)(oct)_2$, **2**; NBE-$CH_2O(CH_2)_5P(O)(oct)_2$, **5**], which are readily obtained by H_2O_2 oxidation of the corresponding phosphines, generate ^{31}P NMR resonances ~70 ppm downfield from the phosphine signals.

Scheme 2. Sequential Polymerization of MTD and Phosphine- or Phosphine Oxide-Functionalized Norbornene Derivatives

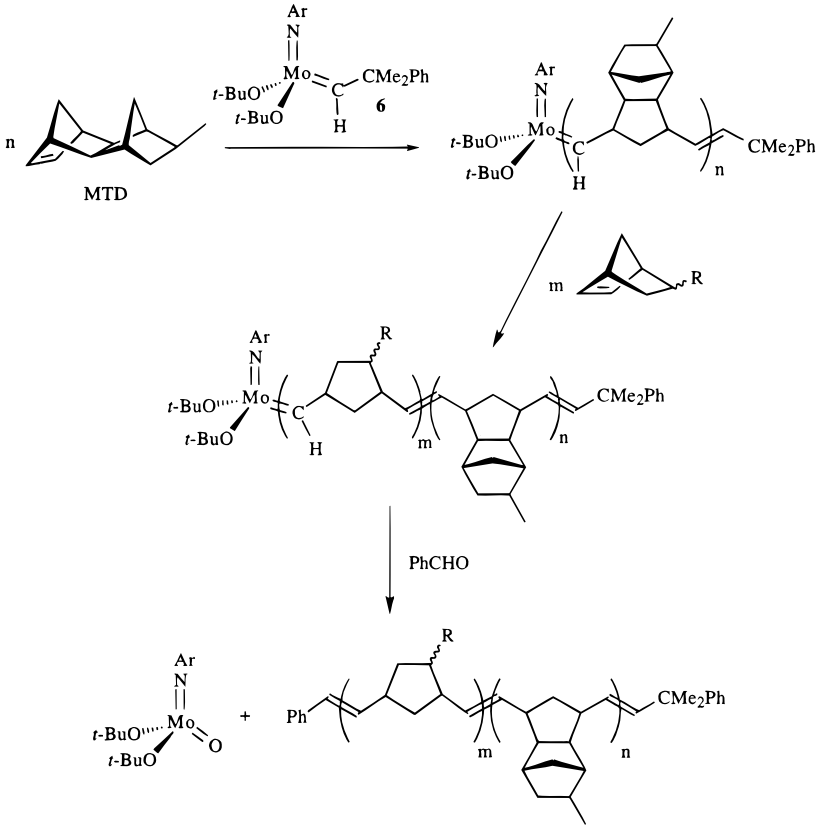

Ar = 2,6-C_6H_3-*i*-Pr_2; R = -$CH_2P(O)(oct)_2$, -$CH_2O(CH_2)_5P(oct)_2$, -$CH_2O(CH_2)_5P(O)(oct)_2$

Polymer Synthesis. Syntheses of MTD homopolymers and MTD-NORPHOS diblock copolymer have been described.[3,15] Homopolymers of MTD are written as $[MTD]_n$, where *n* represents the number of equivalents of monomer used per equivalent of initiator. Almost certainly they do not have regular structures, but probably a mixture of cis and trans double bonds and head-to-head, head-to-tail, and tail-to-tail arrangement of the repeat unit.[8,21] The structure of poly(norbornene) blocks derived from an endo/exo mixture of monosubstituted norbornenes is expected to be similarly complex. The structures given for the polymers therefore are simplified representations.

Polymerizations were carried out in THF, using Mo(CHCMe$_2$Ph)(NAr)(O-*t*-Bu)$_2$ (**6**) as the initiator (Scheme 2). Diblock copolymers were prepared by sequential addition of MTD and the appropriate phosphine-functionalized monomer to the ROMP initiator. Polymerizations were terminated by addition of benzaldehyde, cleaving the polymer chain from the metal in a Wittig-like reaction. Polymers were precipitated by dropwise addition of the concentrated reaction mixture to degassed methanol and analyzed by GPC. As GPC analysis of $[MTD]_{300}$ typically shows a unimodal molecular weight distribution, with a polydispersity index (PDI) of 1.03−1.07, this reaction was used as a periodic check on initiator stability and performance.

NMR studies of the reaction of **6** with several equivalents of NBE-$CH_2P(oct)_2$ (**1**) revealed that **6** was consumed completely, but **1** was not. Chelation of the initially formed alkylidene to give a coordinatively saturated, inactive species, one possible structure of which is shown in eq 2, was inferred from the appearance of ^{31}P NMR singlets due to coordinated phosphorus

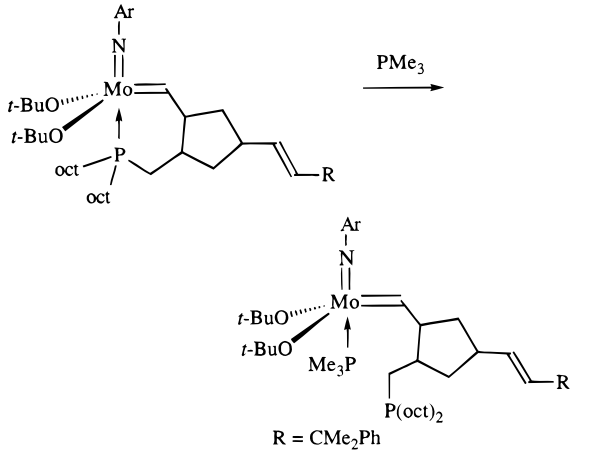

(2)

(δ ∼22, 28). Addition of PMe_3 regenerated the two singlet resonances near −35 ppm due to free **1** as a consequence of displacement of the chelated phosphorus (eq 2). In contrast, NMR studies showed that monomers **2** and **4** (5 equiv) are rapidly and quantitatively polymerized by **6** in C_6D_6. Alkylidene α proton resonances (11.5−11.7 ppm) completely disappeared upon addition of monomer, while olefinic norbornene proton resonances at ∼6.0 ppm were replaced by resonances at ∼5.6 ppm for olefinic protons in the olefin formed upon opening the norbornene ring. No ^{31}P NMR signals for coordinated phosphine or phosphine oxide were observed.

The diminished Lewis basicity of the phosphine oxide functionality, relative to phosphine, probably prevents chelation in the case of **2**. For the long-chain phosphine monomer **4**, entropic factors disfavor chelate formation.

Table 2. Summary of Data for Clusters Incorporated into Polymers

polymer sample	% uptake[a]	$\Delta\lambda_{abs}$[b]	Δ emission[c]	
			37 Å clusters	45 Å clusters
$[MTD]_{300}$	33	2	4	3
$[MTD]_{300}[NORPHOS]_{20}$	100	0		116[d]
$[MTD]_{300}[NBE\text{-}CH_2P(O)(oct)_2]_{20}$	100	6	2	7
$[MTD]_{300}[NBE\text{-}CH_2O(CH_2)_5P(oct)_2]_{20}$	100	0	230	180
$[MTD]_{300}[NBE\text{-}CH_2O(CH_2)_5P(O)(oct)_2]_{20}$	100	6	2	8

[a] Weight fraction of cluster taken up by polymer; initial loading level 20 wt %. [b] Changes in position of λ_{max}(nm) relative to free clusters given for small (37 Å) clusters. Larger (45 Å) clusters exhibit no shift in any of the polymers examined. [c] As percent of initial fluorescence intensity (of free clusters); measured within 30 min of mixing. [d] Drops to 5% of initial value within 12 h.

Copolymers of MTD with monomers **2**, **4**, or **5** were readily prepared by sequential addition of the monomers to initiator **6** (Scheme 2). The timescale of polymerization for **4** was assessed both from in situ NMR experiments and by quenching successive aliquots of a reaction with PhCHO for subsequent ^1H NMR analysis. Formation of the P_{20} block was found to be complete within 1 h.

Polymerization Results. GPC analysis of $[MTD]_{300}$ and $[MTD]_{300}[NORPHOS]_{20}$ indicated narrow, unimodal molecular weight distributions. An unexpected bimodality was observed for the MTD copolymers of **2**, **4**, and **5**, with a variable peak ratio, and an M_n ratio of ~5−10:1. (Peak ratios and M_n values cannot be precisely determined, owing to overlap between the two peaks.) The very narrow PDI values for the peaks (typically <1.06) imply that two distinct initiator species are formed, each giving rise to a living polymer. The observed bimodality is not due to an intrinsic rate difference between Mo−MTD and Mo−phosphine propagating species reacting with the phosphine-containing monomer, as bimodality is retained on reversing the usual order of addition (i.e. adding **4** first, then MTD). The involvement of monomer phosphine as a donor ligand[23] is also improbable; not only would a diminished effect be expected for copolymers of **2** and **5** (in which the Lewis basicity of the auxiliary donor is much attenuated), but a bimodal GPC trace is also found for copolymers of MTD and $NBE\text{-}CH_2O(CH_2)_5Br$. Binding of Br to the metal is unlikely to be significant, as GPC traces of $[MTD]_{300}$ prepared in the presence or absence of $Br(CH_2)_5Br$ were identical.

The origin of the bimodal molecular weight distribution remains unclear despite considerable effort directed at its elucidation. Variation in the proportion of the two GPC peaks between different batches of the same monomer point toward extrinsic factors, rather than an intrinsic property of the monomers. It should be noted that oxygen contamination, which gives rise to a characteristic double molecular weight peak,[24] is ruled out by the high M_n ratio observed. Similarly, trace water (which may convert the initiator to a living, ROMP-active oxo species[25,26] through protonation of the imido functionality) does not appear to be implicated, as rigorous drying of the monomers did not affect the GPC results, while polymerization of MTD in the presence of 1 equiv of degassed water did not give rise to a bimodal GPC trace.

Incorporation of CdSe Nanoclusters into ROMP Polymers. The structural integrity of the clusters was monitored by visible absorption spectroscopy, while electronic passivation was monitored by emission spectroscopy. The extent of cluster uptake was assessed by mixing the clusters and the polymers in THF and then removing the solvent. Extraction of the solid residue with pentane removes any polymer-free clusters. The extent of cluster uptake was then quantified by reference to a Beer's law plot for the relevant cluster batch (Figure 1). Uptake and optical spectroscopy data are summarized in Table 2. Absorption data are listed for small (37 Å) clusters only; the larger clusters (45 Å) are more structurally robust and exhibit no change in absorption spectra upon incorporation into any of the polymers examined. Fluorescence data are reported for both cluster sizes.

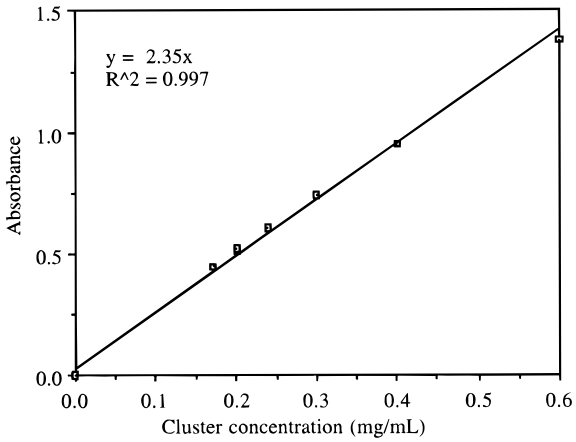

Figure 1. Representative Beer's law plot for ~45 Å clusters: absorbance at 578 nm vs cluster concentration.

Some cluster uptake by MTD homopolymer was observed; it was not accompanied by structural degradation. Uptake by phosphine oxide copolymers was quantitative, but in the case of the smaller clusters, uptake was accompanied by some degradation in cluster size. An immediate decrease in fluorescence was observed for clusters in both $[MTD]_{300}$ and phosphine oxide-containing copolymers. Addition of $P(oct)_3$ to the cluster solutions prior to adding phosphine oxide copolymer limited depassivation, but incorporation was then incomplete. For $[MTD]_{300}[NORPHOS]_{20}$, a small initial increase in fluorescence diminished over 24 h in solution.

Cluster uptake by $[MTD]_{300}[NBE\text{-}CH_2O(CH_2)_5P(oct)_2]_{20}$ was complete, and excellent retention of structural integrity was found, even for 37 Å clusters. Addition of polymer to cluster solutions in all cases resulted in a significant, though variable, increase in fluorescence. Larger increases are found when the cluster sample is relatively poorly passivated. Thus an increase in fluorescence quantum yield (ϕ) of 2% was measured immediately upon addition of polymer to a well-passivated cluster sample (ϕ 9%), but for poorly passivated clusters (ϕ 0.6%), doubling of emission was observed within 30 min of adding polymer. Further increases were noted for the latter as the samples were left to stand (Figure 2), presumably owing to some degree of self-assembly in solution as a consequence of the affinity of polymer phosphine for the cluster surface. Addition of $P(oct)_3$

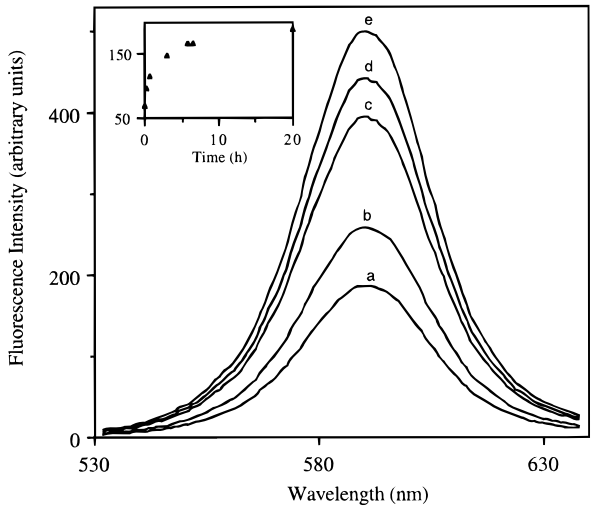

Figure 2. Time-dependence of fluorescence intensity for 37 Å clusters incorporated into $[MTD]_{300}[NBE\text{-}CH_2O(CH_2)_5\text{-}P(oct)_2]_{20}$: (a) emission of free clusters in THF, (b) emission 10 min after adding polymer, (c) after 3 h, (d) after 6 h, (e) after 20 h. Inset shows the increase in fluorescence plotted as a function of time.

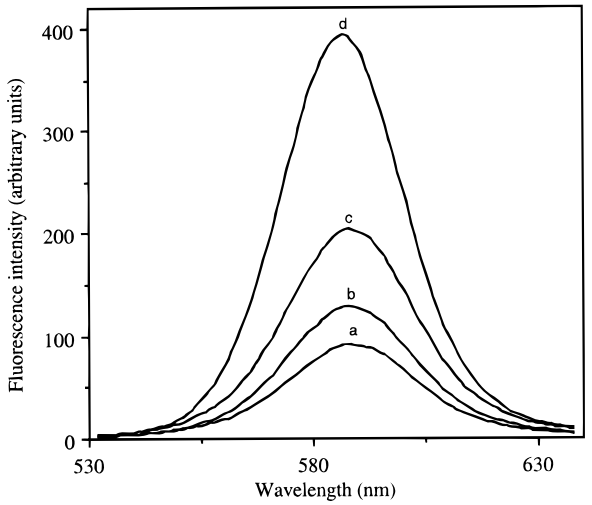

Figure 3. Comparative effects of added $P(oct)_3$ and $O{=}P(oct)_3$ on cluster fluorescence: (a) emission of free clusters in THF, (b) emission after adding 20 μmol $O{=}P(oct)_3$, (c) after adding 0.34 mmol $O{=}P(oct)_3$, (d) after adding 20 μmol $P(oct)_3$.

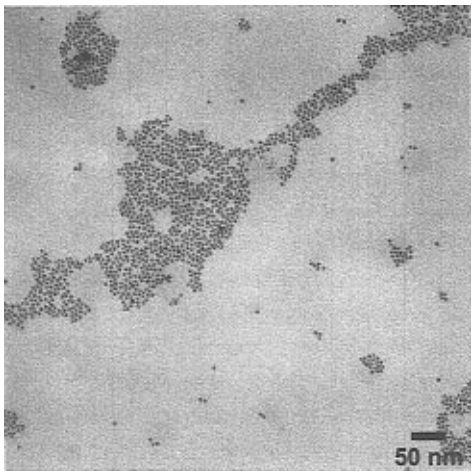

Figure 4. Transmission electron micrograph of 45 Å CdSe nanoclusters in a $[MTD]_{300}$ homopolymer thin film.

after stabilization of the fluorescence signal caused no further increase, implying that repassivation of the cluster surface by polymer-bound phosphine is complete. Fluorescence was furthermore retained in solutions exposed to air for over 3 days, suggesting mutual passivation of the clusters and the otherwise air-sensitive phosphine groups.

Passivation of Clusters by Free $P(oct)_3$ and $O{=}P(oct)_3$. The diminished fluorescence observed upon incorporation of the clusters into phosphine oxide copolymers was unexpected in view of the preference of the cluster surface for phosphine oxide donors inferred from solid state $^{31}P\{^1H\}$ NMR studies of the cluster surface.[27] The effect of added $P(oct)_3$ and $O{=}P(oct)_3$ on the photoluminescence of free clusters therefore was examined. Saturation experiments were conducted in order to determine whether $P(oct)_3$ competes with $O{=}P(oct)_3$ for binding to similar sites on the cluster surface. Addition of successive amounts of $O{=}P(oct)_3$ (up to 0.34 mmol) resulted in successively smaller increases in emission (Figure 3). Subsequent addition of 20 μmol of $P(oct)_3$ resulted in an immediate doubling of the emission (trace d), suggesting that the phosphine is capable of binding to surface sites that are inaccessible to the oxide. Given the greater steric demands of $P(oct)_3$ relative to $O{=}P(oct)_3$ (which would limit access of the former to the surface), these results imply that $P(oct)_3$ can coordinate to Se sites, but the oxide cannot. The much greater passivating effect of phosphine may thus reflect not only the greater affinity of the late transition metals for soft donors such as phosphorus but also the ability of selenium surface sites to bind phosphine, but not phosphine oxide.

It should be noted that these results are not in accord with the model of the cluster surface developed from NMR studies,[27] for which a 30:70 ratio of bound phosphine to phosphine oxide was proposed, with coordination to only cadmium surface sites. The discrepancy perhaps arises from a temperature-dependence in the composition of the passivating layer. Thermal motion may be expected to increase the effective cone angle of the phosphine at high temperatures, limiting the number of such donors which can access the cluster surface. Clusters synthesized at high temperatures, and not subsequently allowed to equilibrate with external added phosphine, may thus have a higher proportion of phosphine oxide capping groups.

TEM Experiments. Thin films of the 45 Å CdSe nanoclusters incorporated into $[MTD]_{300}$ homopolymer, $[MTD]_{300}[NORPHOS]_{20}$, and $[MTD]_{300}[NBE\text{-}CH_2O\text{-}(CH_2)_5P(oct)_2]_{20}$ were examined by TEM. The limited affinity of the nanoclusters for MTD homopolymer noted above is manifest in Figure 4 as the nanoclusters (4.5−5.0 nm in diameter as measured from TEM images) segregate into domains of widely varying size and random arrangement. The nanoclusters are not in direct contact with each other, as the trioctylphosphine caps prevent aggregation. The NORPHOS copolymer shows a similar morphology with a greater, but apparently random, dispersion of nanoclusters over a given area (Figure 5). In contrast, nanoclusters incorporated in $[MTD]_{300}[NBE\text{-}CH_2O(CH_2)_5P(oct)_2]_{20}$ assemble into periodically spaced domains of relatively uniform dimensions and shape. As shown in Figure 6a, the nanoclusters form long and narrow channel-like domains that measure 15−20 nm wide in-plane and are spaced 40−50 nm apart. As periodic long-range order is a hallmark of block copolymer behavior, this morphology is indicative of microphase-separated domains of nanocluster-rich phosphine channels in a poly[MTD]

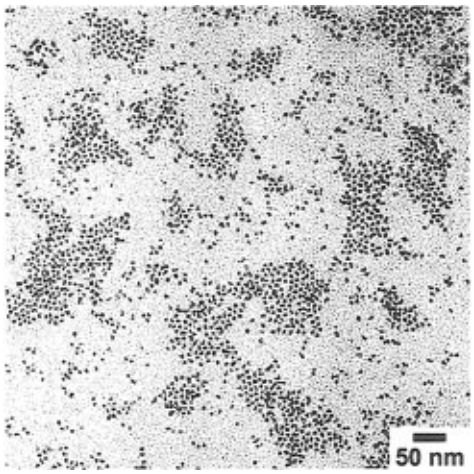

Figure 5. Electron micrograph of 45 Å nanoclusters in a $[MTD]_{300}[NORPHOS]_{20}$ copolymer thin film.

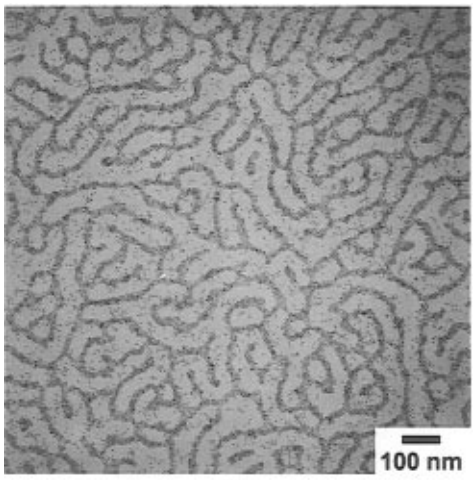

Figure 6. (a) Electron micrograph of 45 Å nanoclusters in a thin film of $[MTD]_{300}[NBE\text{-}CH_2O(CH_2)_5P(oct)_2]_{20}$ copolymer, slow-cast after 30 min equilibration time. (b) Enlarged view of electron micrograph in (a).

matrix. A few, isolated nanoclusters can be seen in the poly[MTD] regions (Figure 6b). The channels also appear to intersect with others at aperiodic intervals to form a network with typically three channels emerging from each junction. A film of similar morphology viewed in cross section (Figure 7) reveals that nanoclusters are encapsulated by the 40 nm thick poly[MTD] matrix. In cross section, the nanocluster-rich domains measure 5−15 nm in the film thickness direction and are coplanar with each other; the network morphology of Figure 6a is thus two-dimensional. In the block copolymer studied here, the poly[MTD] block likely has a lower surface tension with respect to air than the phosphine block, causing the nanocluster-rich domains to be contained within.

The development of the morphology shown in Figure 6a apparently occurs during solvent evaporation. When films were cast in a chamber open to the drybox and without a solvent atmosphere, evaporation of the copolymer solution took place in seconds and produced small aggregates of nanoclusters, 10−20 nm in diameter, with little long range order (Figure 8). Slow evaporation apparently facilitates self-assembly of the component blocks into an ordered morphology, although some self-assembly may occur during equilibration, as the time-dependent increase in fluorescence (Figure 2) would suggest. How close the morphology of Figure 6a is to equilibrium is not known. Formation of equilibrium morphologies in block copolymers is typically accomplished by annealing at temperatures above the glass transition temperatures (T_g) of both component blocks. Annealing at the T_g of the poly[MTD] block (210 °C), however, results in structural degradation of the nanoclusters.

Sections from bulk films of $[MTD]_{300}[NBE\text{-}CH_2O(CH_2)_5P(oct)_2]_{20}$ containing the same relative concentration of nanoclusters reveal a different morphology than in thin films. In order to determine the three-dimensional morphology, sections were ultramicrotomed from three orthogonal faces of the bulk film. As shown in Figure 9, nanoclusters segregate into approximately circular domains, 15−25 nm in diameter and spaced 30−40 nm apart. All sections showed projections similar to Figure 9, indicating that the nanocluster-rich domains are discrete objects. The volume fraction of the phosphine block in this material is 0.14, which corresponds to the sphere morphology in flexible coil diblocks such as polystyrene−polybutadiene. This is consistent with the bulk film, but not the thin films, which exhibit a morphology closer to cylindrical. Differences in morphology between thin and bulk films are not uncommon for block copolymers.[28−30] An attraction for a particular block to the polymer−air or polymer−substrate interface can influence the near-surface morphology, and as film thickness decreases, the constraining effects of both interfaces are felt throughout the film and may cause a transition from the bulk, 3D morphology to a 2D "thin film" morphology.

Finally, the domain dimensions in both thin and bulk films correlate with the sizes of the respective blocks. The unperturbed, root-mean-square, end-to-end distance of the poly[MTD] block is calculated to be 12 nm, which is approximately one-half the width of the poly[MTD] domains in the thin films and therefore suggests a bilayer arrangement of chains. While we do not know the conformations of the phosphine block in the sequestered state, its contour (fully extended) length is 14 nm, which as an upper bound is consistent with the channel width in the thin films.

Discussion

Cluster uptake by MTD homopolymer is presumably due to the lipophilic character of the hydrocarbon tails of the cluster capping groups. The decrease in fluorescence observed on incorporation of the clusters into MTD may arise from disruption of the dynamic equilibrium

Figure 7. Electron micrograph of a nanocluster-containing $[MTD]_{300}[NBE\text{-}CH_2O(CH_2)_5P(oct)_2]_{20}$ thin film viewed in cross section. The surfaces of the film are marked by the dark layers of evaporated carbon which separate the epoxy embedding medium from the copolymer.

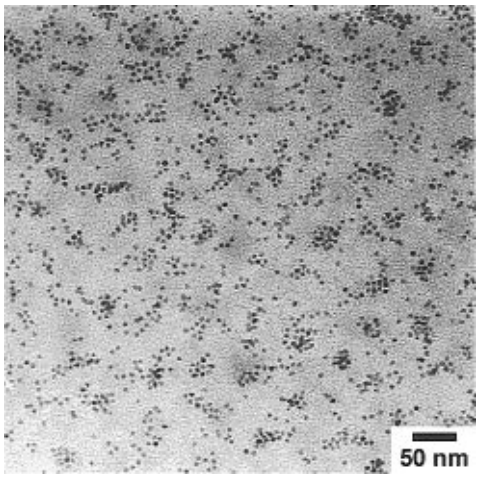

Figure 8. Electron micrograph of 45 Å nanoclusters in a thin film of $[MTD]_{300}[NBE\text{-}CH_2O(CH_2)_5P(oct)_2]_{20}$ copolymer, rapid-cast after 24 h equilibration time.

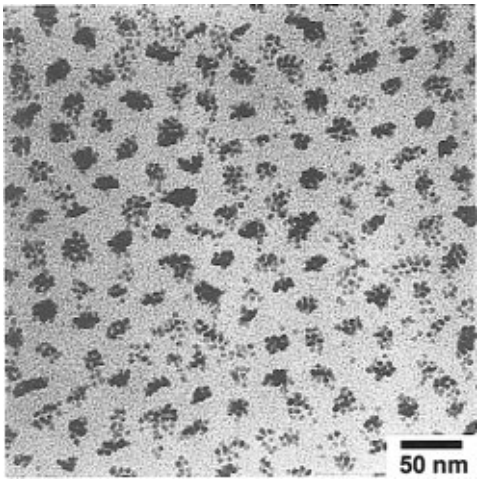

Figure 9. Electron micrograph of 45 Å nanoclusters in an ultramicrotomed section of $[MTD]_{300}[NBE\text{-}CH_2O(CH_2)_5P(oct)_2]_{20}$ bulk film.

between free and bound capping groups by migration of the cluster through the polymer matrix; diffusion constraints may shift the equilibrium in favor of the free ligands. The rather poor affinity of the clusters for NORPHOS copolymers is attributed to the comparatively low Lewis basicity (and hence the low binding affinity) of the diarylphosphine groups, relative to the trialkylphosphine cap. Synthesis of octylphosphine derivatives of norbornene was undertaken in an effort to develop copolymers in which the phosphine block would more effectively mimic the cluster capping groups and securely anchor the clusters to the polymer backbone. While the short-chain monomer **1** could not be polymerized satisfactorily, owing to chelation of the alkylidene to the metal center, no such difficulties are encountered with either the corresponding phosphine oxide **2** or the longer-chain phosphine/phosphine oxide monomers **4** and **5**, and the copolymers are readily prepared. Quantitative cluster uptake is observed by these copolymers (at a 20% w/w loading level of clusters to polymer). Loss of electronic passivation, however, occurs on incorporation of the clusters into any of the phosphine oxide copolymers, despite the slight increase in passivation observed on treatment of free clusters with $O{=}P(oct)_3$. This is probably due to the inability of the comparatively weak phosphine oxide donors to compensate for loss of capping groups resulting from migration of the clusters through the polymer. Incorporation of clusters into phosphine copolymer, in contrast, results in an increase of fluorescence which grows over time, consistent with assembly of the phosphine groups on the cluster surface.

The development of long-range order in $[MTD]_{300}[NBE\text{-}CH_2O(CH_2)_5P(oct)_2]_{20}$ is an interesting aspect of the convergent approach described here. In particular, self-assembly evidently occurs in a two-step process; nanoclusters are sequestered in solution and form small, micelle-like aggregates, followed by microphase separation of the aggregates into periodically spaced domains upon solvent evaporation. Issues that remain unexplored include the effect of the nanoclusters on the ordered morphology of the neat block copolymer, the paths of phosphine chains in the ordered domains and how they are affected by chain architecture, and the dependence of morphology on the relative volume fraction of blocks. Understanding of these details could help in the tailoring of morphologies for specific applications.

Both absorption and TEM data demonstrate that the structural integrity of the originally near-monodisperse nanocluster samples is not compromised by incorporation into the polymer matrix, while the fluorescence results indicate that electronic passivation is not merely maintained but is in fact enhanced in the composite materials. These results thus represent some of the most successful efforts to date at fabrication of nanostructured polymer−cluster composites, in which highly monodisperse, electronically passivated semiconductor clusters are localized within one domain of a diblock copolymer. These materials offer significant advances in the controlled placement and anchoring of clusters within a polymer matrix, and experiments directed at exploiting these abilities are under way. Our current efforts focus on the development of alternative matrix blocks and exploration of the electron-transport properties of the modified materials.

Acknowledgment. This work was supported by the National Science Foundation (Grant DMR 87 19217) and in part by the MRSEC Program of the National Science Foundation under award number DMR 94-00334. We thank M. G. Bawendi for useful discussions and the B.F. Goodrich Co. for a generous supply of MTD.

References and Notes

(1) Yuan, Y.; Fendler, J. H.; Cabasso, I. *Chem. Mater.* **1992**, *4*, 312.

(2) Wozniak, M. E.; Sen, A.; Rheingold, A. L. *Chem. Mater.* **1992**, *4*, 753.
(3) Chan, Y. N. C.; Schrock, R. R.; Cohen, R. E. *J. Am. Chem. Soc.* **1992**, *114*, 7295.
(4) Wang, Y.; Herron, N. *Chem. Phys. Lett.* **1992**, *200*, 71.
(5) Schueller, O. J. A.; Pocard, N. L.; Huston, M. E.; Spontak, R. J.; Neenan, T. X.; Callstrom, M. R. *Chem. Mater.* **1993**, *5*, 11.
(6) Fréchet, J. M. J.; Golden, J. H.; Deng, H.; DiSalvo, F. J.; Thompson, P. M. *Science* **1995**, *268*, 1463.
(7) Murray, C. B.; Norris, D. J.; Bawendi, M. G. *J. Am. Chem. Soc.* **1993**, *115*, 8706.
(8) Schrock, R. R. In Ring-Opening Polymerization; Brunelle, D. J., Ed.; Hanser: Munich, 1993.
(9) Schrock, R. R.; Lee, J.-K.; O'Dell, R.; Oskam, J. H. *Macromolecules* **1995**, *28*, 5933.
(10) Schrock, R. R. *Polyhedron* **1995**, *14*, 3177.
(11) Oskam, J. H.; Schrock, R. R. *J. Am. Chem. Soc.* **1993**, *115*, 11831.
(12) Yue, J.; Sankaran, V.; Cohen, R. E.; Schrock, R. R. *J. Am. Chem. Soc.* **1993**, *115*, 4409.
(13) Chan, Y. N. C.; Schrock, R. R. *Chem. Mater.* **1993**, *5*, 566.
(14) Chan, Y. N. C.; Craig, G. S. W.; Schrock, R. R.; Cohen, R. E. *Chem. Mater.* **1992**, *4*, 885.
(15) Chan, Y. N. C.; Schrock, R. R.; Cohen, R. E. *Chem. Mater.* **1992**, *4*, 24.
(16) Cummins, C. C.; Schrock, R. R.; Cohen, R. E. *Chem. Mater.* **1992**, *4*, 27.
(17) Schrock, R. R.; Murdzek, J. S.; Bazan, G. C.; Robbins, J.; DiMare, M.; O'Regan, M. *J. Am. Chem. Soc.* **1990**, *112*, 3875.
(18) Brunner, H.; Pieronczyk, W. *Angew. Chem., Int. Ed. Engl.* **1979**, *18*, 620.
(19) Horner, L.; Hoffman, H.; Beck, P. *Chem. Ber.* **1958**, *91*, 1583.
(20) Hill, E. A.; Hsieh, K.; Condroski, K.; Sonnentag, H.; Skalitzky, D.; Gagas, D. *J. Org. Chem.* **1989**, *54*, 5286.
(21) Schrock, R. R. *Acc. Chem. Res.* **1990**, *24*, 158.
(22) Katari, J. E. B.; Colvin, V. L.; Alivisatos, A. P. *J. Chem. Phys.* **1994**, *98*, 4109.
(23) Wu, Z.; Wheeler, D. R.; Grubbs, R. H. *J. Am. Chem. Soc.* **1992**, *114*, 146.
(24) Feast, W. J.; Gibson, V. C.; Khosravi, E.; Marshall, E. L.; Mitchell, J. P. *Polymer* **1992**, *33*, 872.
(25) O'Donoghue, M. B.; Schrock, R. R.; LaPointe, A. M.; Davis, W. M. *Organometallics* **1996**, *15*, 1334.
(26) de la Mata, F. J.; Grubbs, R. H. *Organometallics* **1996**, *15*, 577.
(27) Becerra, L.; Murray, C. B.; Griffin, R. G.; Bawendi, M. G. *J. Chem. Phys.* **1994**, *100*, 3297.
(28) Krausch, G. *Mater. Sci. Engin.* **1995**, ***R14***, 1.
(29) Henkee, C. S.; Thomas, E. L.; Fetters, L. J. *J. Mater. Sci.* **1988**, ***23***, 1685.
(30) Radzilowski, L. H.; Carvalho, B. C.; Thomas, E. L. *J. Polym. Sci., Polym. Phys.* **1996**, *34*, 3081.

MA961103Y